Int. J. Electrochem. Sci., 10 **(2015)** 659 - 670

International Journal of
ELECTROCHEMICAL
SCIENCE
www.electrochemsci.org

Study of Electrochemical Deposition and Degradation of Hydroxyapatite Coated Iron Biomaterials

Renáta Oriňaková[1,*], *Andrej Oriňak*[1], *Miriam Kupková*[2], *Monika Hrubovčáková*[2], *Lenka Škantárová*[1], *Andrea Morovská Turoňová*[1], *Lucia Markušová Bučková*[1], *Christian Muhmann*[3], *Heinrich F. Arlinghaus*[3]

[1] Department of Physical Chemistry, Faculty of Science, P.J. Šafárik University, Moyzesova 11, SK-04154 Košice, Slovak Republic
[2] Institute of Materials Research, Institute of Material Research, Slovak Academy of Science, Watsonova 47, SK-04353 Košice, Slovak Republic
[3] Institute of Electrical Engineering, Slovak Academy of Sciences, Dúbravská cesta 9 SK-841 04 Bratislava, Slovak Republic
4Physical Institute, Wilhelm Westphalen University, Wilhelm-Klemm-Strasse 10, D-48149 Muenster, Germany
[*]E-mail: Renata.Orinakova@upjs.sk

Received: 10 October 2014 / *Accepted:* 15 November 2014 / *Published:* 2 December 2014

The sintered iron samples were electrochemically coated with hydroxyapatite (HAp) and manganese-doped HAp (MnHAp) ceramics layer to enhance the biocompatibility of biodegradable material for orthopaedic applications. The influence of electrodeposition duration and concentration of Mn^{2+} ions in the electrolyte on the amount, surface appearance, composition and corrosion properties of developed samples was studied. The surface morphology was examined using a scanning electron microscope (SEM) and energy-dispersive X-ray (EDX) analysis. Formation of HAp was proved by time of flight secondary ion mass spectrometry (TOF SIMS). The corrosion behaviour was investigated by means of potenciodynamic polarisation measurements in Hank's solution. Amount of MnHAp coating was lower than the amount of HAp coating deposited at the identical deposition conditions. Introduction of Mn into the bioceramic film resulted in different surface morphology. The increase in Mn content in MnHAp coating at higher concentration of Mn^{2+} ions in deposition bath and longer deposition time was observed. Moreover, the higher content of P and Ca in bioceramic films at longer deposition time was detected. The slight decrease in corrosion susceptibility due to the presence of bioceramic coating layer was registered. The lowest degradation rate was observed for iron sample with HAp coating layer.

Keywords: carbonyl iron, powder metallurgy, hydroxyapatite, electrodeposition, corrosion behaviour

1. INTRODUCTION

The development of non-toxic and allergy-free biomaterials is one of the most important directions of material chemistry today [1]. Degradable metallic implants have achieved clear advantages in orthopedic applications in the last few years, because of their biocompatibility, high strength and high elastic modulus [2-6]. Iron plays very important role in human body metabolism, but some difficulties arise when this material is used for surgical implants due to the ferromagnetic behavior and the slow degradation rate of pure Fe [7-10]. Compared with Mg based alloys, pure iron and its alloy possess better mechanical properties and don't have hydrogen evolution during the degradation [11, 12].

Orthopedic implants usually come in direct contact with bone marrow stromal cells [13]. Therefore, metallic implants are frequently covered with osteoconductive biomaterials, such as hydroxyapatite (HAp) ceramics [14]. HAp is one of the most effective bioceramics in the clinical repair of hard-tissue injury and illness [15]. It possesses excellent biocompatibility, both in-vitro and in-vivo [16] and it is also degradable in body environment [17]. HAp is the major mineral component of human hard tissues composed of calcium, phosphate and hydroxyl ions with Ca/P ratio within the range known to promote bone regeneration (1.50 - 1.67) [18-20]. Moreover, the hybrid manganese-doped HAp (MnHAp) material was shown to greatly improve the quality and rate of bone repair in biocoating technology [21-24]. The addition of Mn^{2+} into HAp coating significantly reduced the porosity, induces its interaction with the host bone tissue, improves the ligand binding affinity of integrins, and activates cellular adhesion [22-27].

The iron biodegradable materials were proved to be suitable biomaterials for cardiovascular and orthopaedic applications [8-10, 28]. However, the observed degradation rate was rather low. For this reason, the incoherent thin HAp layer was deposited on the surface of iron substrate and the effect of this layer on corrosion behaviour in simulated body fluid was evaluated in this work. Addition of Mn to HAp was examined for their ability to increase biocompatibility and degradation rate of biomaterials. Electrochemical deposition of HAp coatings is favourable due to the availability and low cost, the ability to coat complex shape or porosive substrates and, the ability to control coating properties by adjusting the deposition conditions [1, 18, 19, 22]. The effect of deposition time and concentration of Mn^{2+} ions in the electrolyte solution on surface morphology, amount and composition of deposited bioceramic layer was studied.

2. EXPERIMENTAL PART

2.1 Materials preparation

The carbonyl iron powder (CIP) fy BASF (type CC, d50 value 3.8 – 5.3 μm) with composition: 99.5 % Fe, 0.05 % C, 0.01 % N and 0.18 % O used for the experiments as a starting material was cold pressed at 600 MPa into pellets (Ø 10 mm, h 2 mm) and sintered in a tube furnace for 1 hour at 1120°C in reductive atmosphere (10 % H_2 and 90 % N_2).

2.2 Electrodeposition of HAp and MnHAp coating layers

The surface of prepared Fe plates was finished gradually with SiC papers of different grits (240, 800 and 1500). Then, the surface was ultrasonically washed in acetone, anhydrous ethanol and distilled water.

Cathodic electrochemical deposition ED was carried out using an Autolab PGSTAT 302N potentiostat and conventional three-electrode system with the Ag/AgCl/KCl (3 mol/l) reference electrode, platinum counter electrode and Fe pellet as the working electrode. Deposition of HAp layer was realised in an electrolyte composed of 4.2 x 10^{-2} mol/l $Ca(NO_3)_2$ (analytical grade), 2.5 x 10^{-2} mol/l $NH_4H_2PO_4$ (analytical grade). Deposition of MnHAp layer was conducted from the same electrolyte with addition of 3 x 10^{-4} mol/l or 3 x 10^{-3} mol/l $Mn(NO_3)_2$ (analytical grade) under the following parameters: pH 4.3 ± 0.5, current density 0.85 mA cm^{-2}, deposition time 20 or 40 min and temperature 65 ± 0.5 °C. After deposition, the samples were immersed in 1 mol/l NaOH solution at 65 ^oC for approximately 2 h, washed in distilled water and then dried at 80 ^oC for 2 h. Then, the samples were sintered at 400 °C for 2 h in N_2.

2.3 Materials characterization

The microstructure of the experimental specimens was observed by a scanning electron microscope (SEM) (JOEL JSM-7001F, Japan equipped with INCA EDX analyzer).

Time of flight secondary ion mass spectrometry (TOF SIMS) experiments were performed with a TOF SIMS IV instrument built at University of Münster by using a 25 keV Bi_3^+ primary ions (0.05 pA current). The primary ion beam was rastered on a field of 150 × 150 μm^2 with 256 × 256 pixels and 250 scans. The cycle time was 100 µs. The charge compensation was used.

The content of Mn in MnHAp coating was determined after dissolution in nitric acid by atomic absorption spectrometry (AAS) PERKIN-ELMER 420.

2.4 Electrochemical corrosion measurements

The electrochemical studies were conducted using an Autolab PGSTAT 302N potentiostat, interfaced to a computer. Measurements were carried out by conventional three-electrode system with the Ag/AgCl/KCl (3 mol/l) reference electrode, platinum counter electrode and uncoted or bioceramic coated Fe sample as the working electrode. The degradation behavior was investigated by Hank's solution with a pH value of 7.4 prepared using laboratory grade chemicals and double distilled water. The composition of the Hank's solution used was: 8 g/l NaCl, 0.4 g/l KCl, 0.14 g/l $CaCl_2$, 0.06 g/l $MgSO_4.7H_2O$, 0.06 g/l $NaH_2PO_4.2H_2O$, 0.35 g/l $NaHCO_3$, 1.00 g/l Glucose, 0.60 g/l KH_2PO_4 and 0.10 g/l $MgCl_2.6H_2O$. Freshly prepared solution was used for each experiment. A constant electrolyte temperature of 37±2°C was maintained using a heating mantle. All the potentiodynamic polarization studies were conducted after stabilization of the free corrosion potential. The potentiodynamic polarization tests were carried out from -800 mV to -200 mV (vs. Ag/AgCl/KCl (3 mol/l)) at a

scanning rate of 0.1 mV/s. The corrosion rate was determined using the Tafel extrapolation method. The corrosion rate (*CR*) was calculated using equation:

$$CR = \frac{j_{corr}\, K\, EW}{d} \qquad (1)$$

where, j_{corr} is current density (A/cm^2), *EW* is equivalent weight (g/mol), *d* is density (g/cm^3) and *K* is a constant that defines the units for the corrosion rate.

3. RESULTS AND DISCUSSION

3.1. Cathodic deposition of bioceramic coating layer

Cathodic electrochemical deposition of HAp layer was performed in an electrolyte solution containing 4.2 x 10^{-2} mol/l $Ca(NO_3)_2$ and 2.5 x 10^{-2} mol/l $NH_4H_2PO_4$ for 20 min and 40 min. Electrodeposition of MnHAp films was conducted from the same electrolyte with addition of 3 x 10^{-4} mol/l or 3 x 10^{-3} mol/l $Mn(NO_3)_2$ for 20 min and 40 min.

The mechanism of cathodic electrochemical deposition of HAp coating was early reported on different substartes [18, 22, 29, 30]. The following electrochemical and chemical reactions are involved in the deposition of HAp and MnHAp coatings:

$$2\,H^+ + 2\,e^- \rightarrow H_2 \qquad (2)$$

$$O_2 + 2\,H_2O + 4\,e^- \rightarrow 4\,OH^- \qquad (3)$$

$$2\,H_2O + 2\,e^- \rightarrow H_2 + 2\,OH^- \qquad (4)$$

$$NO_2 + 2\,H_2O + 4\,e^- \rightarrow 4\,OH^- \qquad (5)$$

$$NO_3^- + H_2O + 2e^- \rightarrow 2\,OH^- + NO_2^- \qquad (6)$$

$$H_2PO_4^- + H_2O + 2e^- \rightarrow 2\,OH^- + H_2PO_3^- \qquad (7)$$

$$H_2PO_4^- + OH^- \rightarrow H_2O + HPO_4^{2-} \qquad (8)$$

$$H_2PO_4^- + e^- \rightarrow HPO_4^{2-} + \tfrac{1}{2}\,H_2 \qquad (9)$$

$$H_2PO_4^- + 2\,e^- \rightarrow PO_4^{3-} + H_2 \qquad (10)$$

$$H_2PO_4^- \rightleftarrows HPO_4^{2-} + H^+ \qquad (11)$$

$$HPO_4^{2-} + OH^- \rightarrow H_2O + PO_4^{3-} \qquad (12)$$

$$HPO_4^{2-} + e^- \rightarrow \tfrac{1}{2}\,H_2 + PO_4^{3-} \qquad (13)$$

$$Ca^{2+} + HPO_4^{2-} + 2\,H_2O \rightarrow CaHPO_4 \times 2\,H_2O \qquad (14)$$

$$x\,Mn^{2+} + (1-x)\,Ca^{2+} + HPO_4^{2-} + 2\,H_2O \rightarrow Mn_xCa_{(1-x)}HPO_4 \times 2\,H_2O \quad (1>x>0) \qquad (15)$$

$$3\,Ca^{2+} + PO_4^{3-} \rightarrow Ca_3(PO_4)_2 \qquad (16)$$

The hydroxyl ions formed through reactions (3) – (7) the leads to the increase in concentration of phosphate ions and subsequently resulted in deposition of HAp.

Following reactions represent the formation of hydroxyapatite films resulted from the alkaline treatment to the coated samples [22, 29]:

$$10\,CaHPO_4 \times 2\,H_2O + 12\,OH^- \rightleftarrows Ca_{10}(PO_4)_6(OH)_2 + 4\,PO_4^{3-} + 30\,H_2O \qquad (17)$$

$$10\,Mn_xCa_{(1-x)}HPO_4 + 2\,OH^- \rightarrow Mn_{10x}Ca_{(10-10x)}(PO_4)_6(OH)_2 + 4\,PO_4^{3-} + 10\,H^+ \quad (1>x>0) \qquad (18)$$

The formation of HAp and MnHAp coating layers was confirmed by TOF SIMS, SEM and EDX studies.

3.2. SEM and EDX analysis of bioceramic coating layer

Representative SEM images of the surface of uncoated sintered iron sample and bioceramic coated iron samples are shown in Fig. 1. The incoherent HAp layer consisting of flake-like star-shaped structures on the iron surface could be seen in Figs 1b and 1c as compared to smooth surface of uncoated iron sample (Fig. 1a). The unhomogeneously distributed cracked MnHAp coating layers with globular irregular structures are shown in Figs. 1d and 1e. Neither the deposition time nor the concentration of Mn^{2+} ions have changed the surface appearance of bioceramic layer. All deposited coatings were stable and very adhesive.

Table 1. Mass of bioceramic coating layer determined from the mass difference of coated and uncoated samples depending on the deposition time and concentration of $Mn(NO_3)_2$ in the electrolyte.

Deposition time / min	Mass of bioceramic coating layer / mg		
	HAp	MnHAp	
		3x 10^{-4} mol/l $Mn(NO_3)_2$	3x 10^{-3} mol/l $Mn(NO_3)_2$
20	3.4 ± 0.4	2.2 ± 0.3	2.2 ± 0.5
40	3.6 ± 0.4	2.3 ± 0.4	2.4 ± 0.3

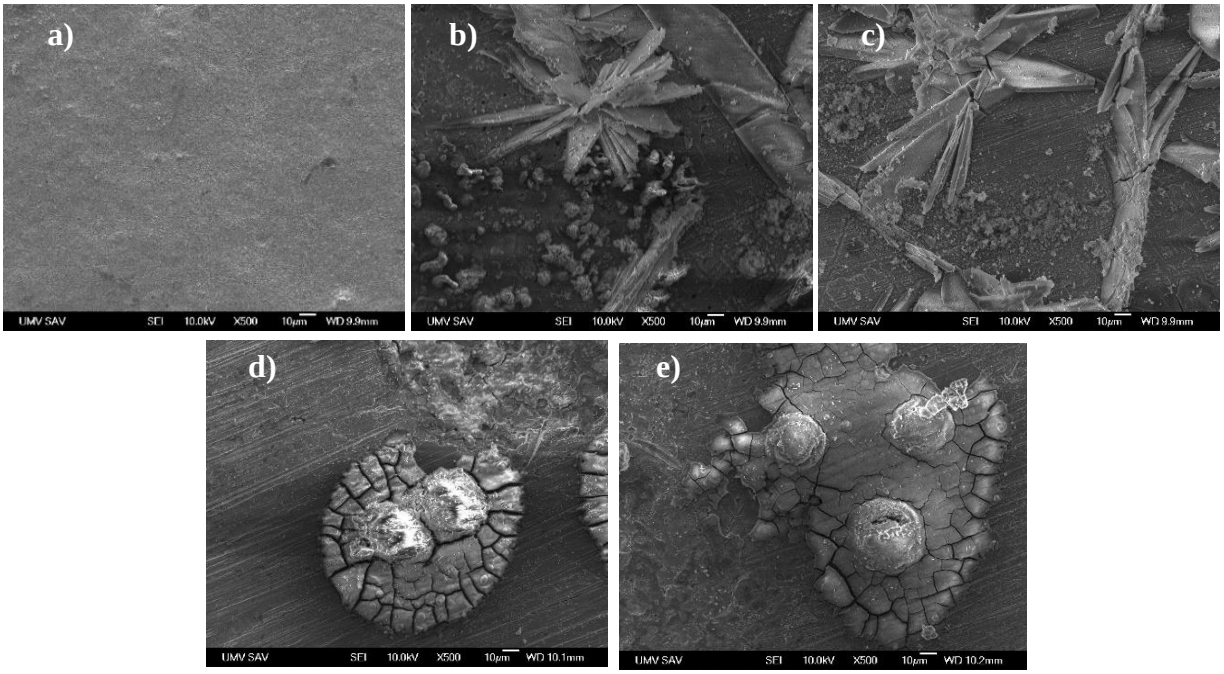

Figure 1. SEM images of the surface of uncoated Fe substrate (a), Fe material with HAp layer at 20 min (b) and 40 min (c), and Fe material with MnHAp layer deposited from the electrolyte containing 3 x 10-3 M Mn(NO3)2 at 20 min (d) and 40 min (e).

The amount of deposited bioceramic coating layers determined from the mass difference of coated and uncoated cylindrical iron samples are summarised in Table 1. Again, neither the deposition time nor the concentration of Mn^{2+} ions have affected significantly the mass of deposited bioceramic coating. Generally, amount of MnHAp coating was lower than the amount of HAp coating deposited at the same deposition conditions.

Content of Mn in MnHAp hybrid layer determined by AAS after the removal and dissolution of coating layer was between 0.2 and 0.3 wt.% for lower concentration of Mn^{2+} and between 0.4 and 0.5 wt.% for higher concentration of Mn^{2+}.

The elemental analyses performed by EDX on the surface of sintered iron samples coated with HAp layer revealed the difference in the composition of layers deposited at different deposition times. Average composition of the surface of sintered iron samples with HAp coating layer depending on the deposition time calculated form cca 10 EDX analyses performed on different areas of the surface are referred in Table 2. Content of P and Ca was higher while the content of Fe and O was lower in the HAp layer deposited after 40 min as compared to the HAp layer deposited after 20 min.

Table 2. Nominal composition of the surface of sintered iron samples with HAp coating layer depending on the deposition time.

Element	Average composition of Fe sample with HAp / %			
	20 min		40 min	
	wt.%	at.%	wt.%	at.%
C K	2.52	6.07	2.70	6.53
O K	26.91	48.79	23.67	43.01
Na K	2.33	2.95	2.20	2.79
P K	8.37	7.84	12.50	11.74
Ca K	15.96	11.55	25.68	18.63
Fe K	43.90	22.80	33.26	17.32

Table 3. Nominal composition of the surface of sintered iron samples with MnHAp coating layer depending on the deposition time and concentration of Mn^{2+} ions.

Element	Average composition / %							
	3x 10^{-4} mol/l $Mn(NO_3)_2$				3x 10^{-3} mol/l $Mn(NO_3)_2$			
	20 min		40 min		20 min		40 min	
	wt.%	at.%	wt.%	at.%	wt.%	at.%	wt.%	at.%
C K	3.92	9.95	4.22	9.26	3.41	8.66	8.06	15.20
O K	24.23	46.23	28.94	47.74	23.38	47.59	35.48	50.22
Na K	2.59	2.97	3.72	4.65	1.97	1.53	4.34	4.22
P K	3.49	3.44	11.21	9.55	3.56	3.53	10.42	7.61
Ca K	6.40	4.88	21.45	14.13	6.54	5.01	21.24	12.00
Mn K	2.67	1.54	3.21	1.78	3.27	1.83	10.16	4.19
Fe K	56.70	30.99	27.24	12.87	57.86	31.84	10.30	6.56

The increase in the content of P and Ca with increasing deposition time was observed also for MnHAp coating. Moreover, the increase in Mn content in MnHAp layer with increasing deposition time as well as with increasing concentration of Mn^{2+} ions was detected. Average composition of the surface of sintered iron samples with MnHAp coating layer depending on the deposition time and $Mn(NO_3)_2$ concentration calculated form EDX analyses are summarised in Table 3.

3.3. TOF SIMS analysis of bioceramic coating layer

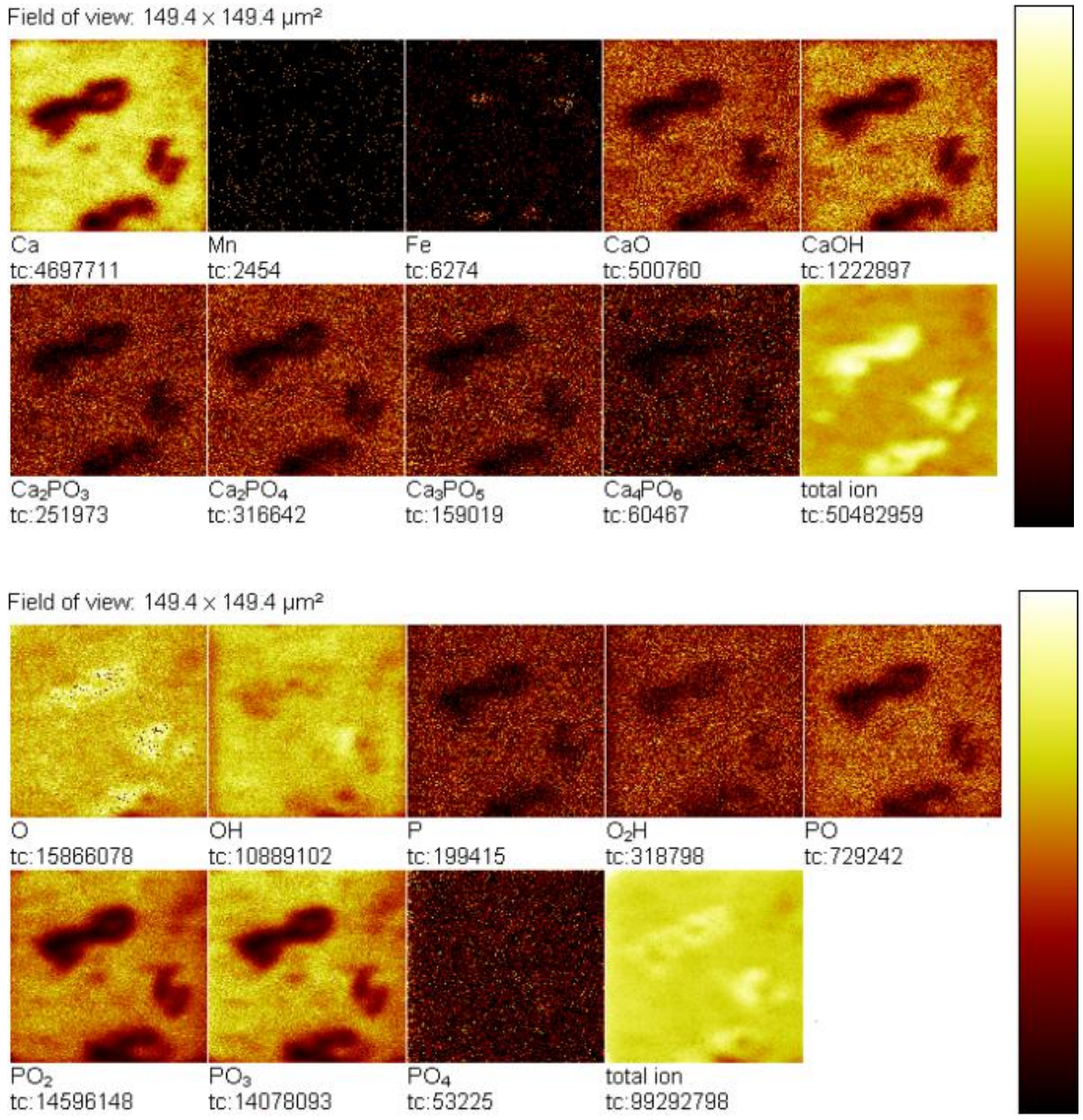

Figure 2. 2D distribution of characteristic fragments of HAp coated Fe sample surface obtained by TOF SIMS analysis: positive mode (upper), negative mode (bottom). The deposition time was 40 min.

The presence of HAp in bioceramic coating layers was later confirmed by TOF SIMS analysis. As TOF SIMS is a purely surface sensitive technique in the static mode, thus only the uppermost molecular layers are analysed [31]. The representative TOF SIMS images of HAp and MnHAp coated iron samples recorded in the positive and negative ion modes are presented in Fig. 2 and Fig. 3, respectively.

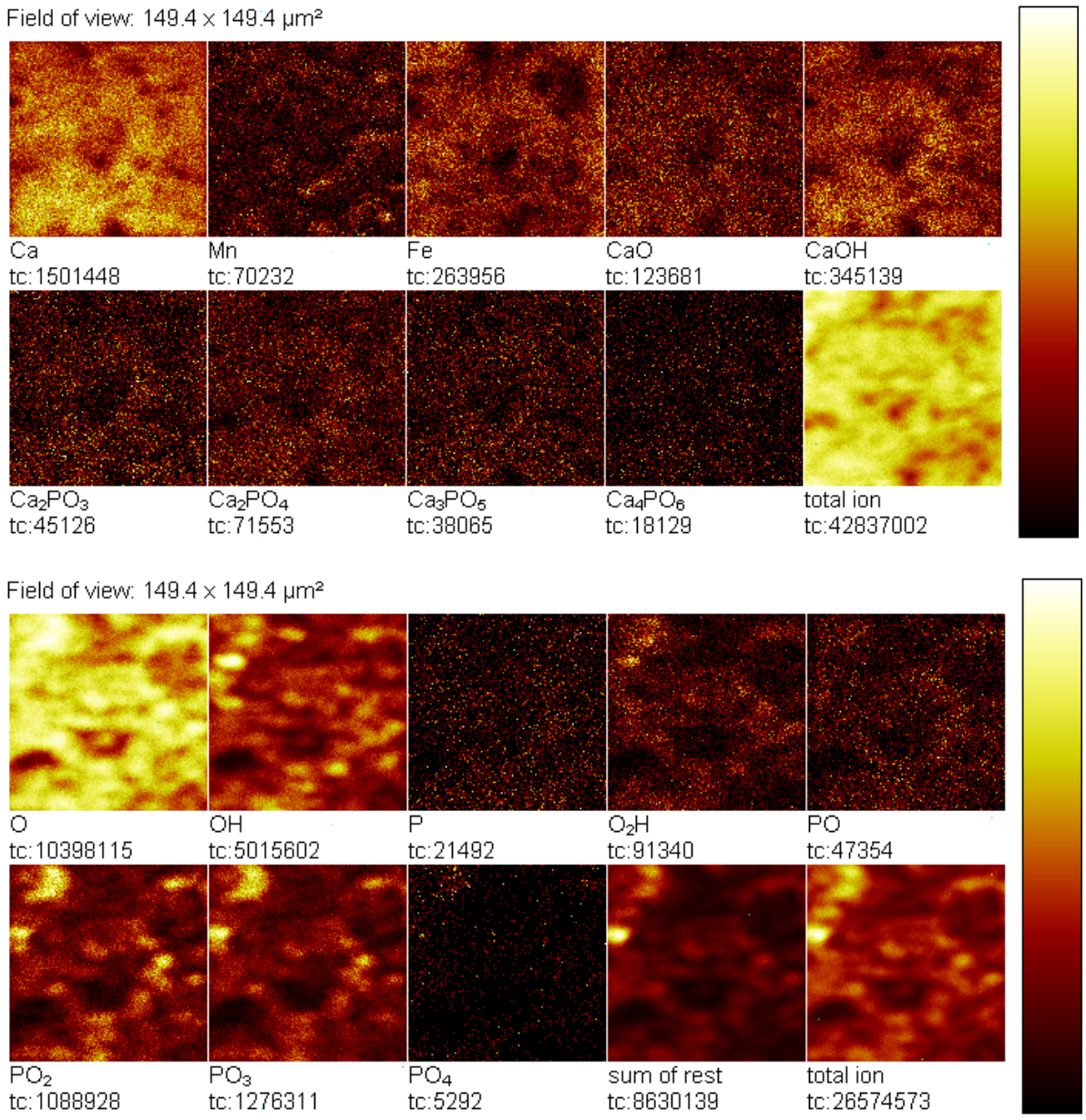

Figure 3. 2D distribution of characteristic fragments of MnHAp coated Fe sample surface obtained by TOF SIMS analysis: positive mode (upper), negative mode (bottom). The deposition time was 40 min, concentration of $Mn(NO_3)_2$ was 3x 10^{-3} mol/l.

Characteristic positive fragment ions derived from a $Ca_{10}(PO_4)_6(OH)_2$ precursor species allowing its identification include Ca^+, CaO^+, $CaOH^+$, Ca_2PO_3, Ca_2PO_4 and Ca_3PO_5. Characteristic

negative fragment ions include O^-, OH^-, P^-, HO_2^-, PO^-, PO_2^-, PO_3^- and PO_4^-. [31, 32]. Generally, intensities of characteristic fragment ions were higher for HAp coating than for MnHAp layer which could be assigned to the higher amount of HAp as compared to MnHAp. The $CaOH^+/Ca^+$ (57/40) fragments intensity ratio have often been used to identify different calcium phosphates. The values of $CaOH^+/Ca^+$ intensity ratios we observed were 0.26 ± 0.01 for HAp and 0.24 ± 0.01 for MnHAp coating layer. Similar results were previously obtained by Yan et al. [33] and França et al. [34].

3.4 Electrochemical corrosion test

Representative potentiodynamic polarisation curves obtained from the uncovered and bioceramic coated Fe samples in Hank's solution at 37 °C are shown in Fig. 4. The corrosion potential (E_{corr}) and corrosion current density (j_{corr}) were calculated from the intersection of the anodic and cathodic Tafel lines extrapolation. The reproducibility of Tafel plots was good. The values of E_{corr}, j_{corr} and average corrosion rates extracted from potentiodynamic polarisation curves using polarisation resistance method for three experimental materials are listed in Table 4.

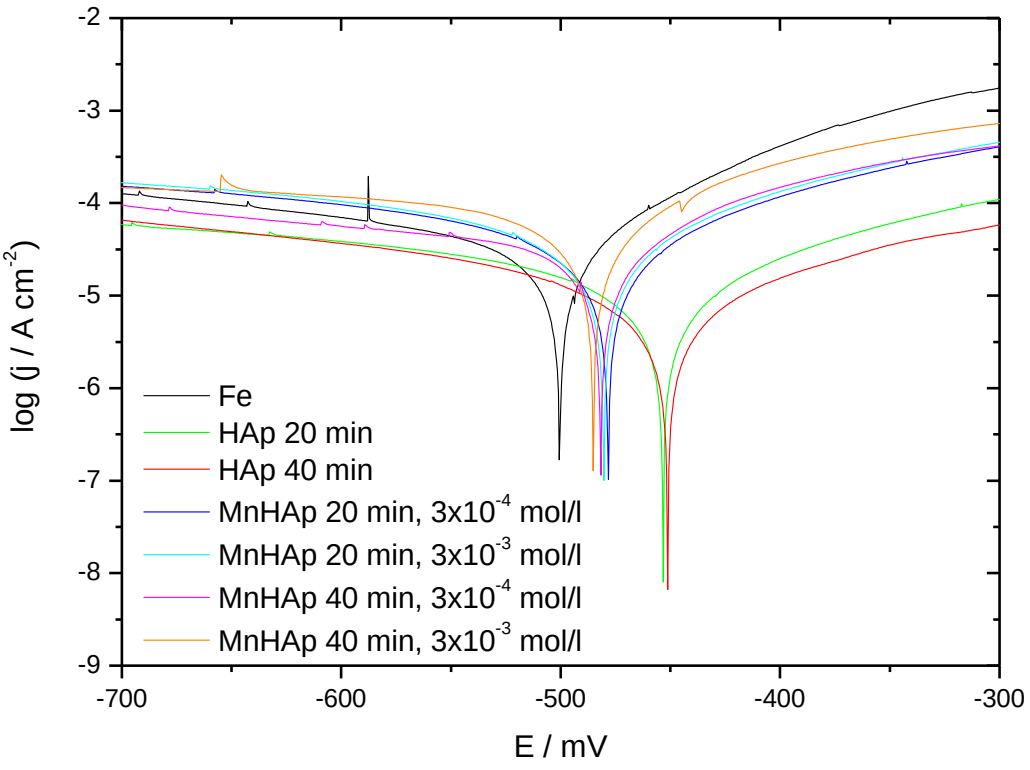

Figure 4. Potentiodynamic polarisation curves of uncoated and bioceramic coated Fe substrate obtained in Hank's solution at pH 7.4 and 37°C at scan rate 0.1 mV/s.

The presence of MnHAp coating layer on the surface of iron sample resulted in slight positive shift of corrosion potential and decrease in corrosion current density as compared to uncoated iron sample. The next positive shift of corrosion potential and decrease in corrosion current density was observed for the iron sample with HAp coating layer. The higher corrosion susceptibility of MnHAp coated samples than that of HAp coated samples was clearly associated with the presence of Mn in the bioceramic layer. Corrosion resistance of MnHAp coated samples decreased with increasing content of Mn in MnHAp coating layer (Tab. 1). The in-vitro degradation rates in Hank's solution determined from potentiodynamic polarisation curves were in the sequence: Fe, MnHAp (40 min, $3x10^{-3}$ mol/l Mn^{2+}), MnHAp (40 min, $3x10^{-4}$ mol/l Mn^{2+}), MnHAp (20 min, $3x10^{-3}$ mol/l Mn^{2+}), MnHAp (20 min, $3x10^{-4}$ mol/l Mn^{2+}), HAp (20 min), HAp (40 min) from higher to lower. The opposite trend was observed for corrosion potentials of developed materials.

Table 4. Values of E_{corr}, j_{corr} and corrosion rates for uncoated and bioceramic coated sintered iron samples obtained from the potentiodynamic polarization curves in Hank's solution at pH 7.4 and 37°C.

	Fe	Fe + HAp		Fe + MnHAp			
				$3x\ 10^{-4}$ mol/l $Mn(NO_3)_2$		$3x\ 10^{-3}$ mol/l $Mn(NO_3)_2$	
Deposition time		20 min	40 min	20 min	40 min	20 min	40 min
E_{corr} (mV)	-502.46	-453.44	-451.75	-478.40	-480.12	-482.50	-485.56
j_{corr} ($\mu A/cm^2$)	46.027	14.724	14.675	21.570	21.971	25.832	28.961
Corrosion rate (mm/year)	0.5348	0.1712	0.1705	0.2506	0.2555	0.2903	0.3364

4. CONCLUSIONS

The adhesive incoherent bioceramic coating was produced by electrochemical deposition on the surface of sintered iron substrates. The flake-like structure of HAp coating layer was changed after addition of Mn to more layered cracked surface appearance of MnHAp film. Amount of both bioceramic coatings as well as the content of P, Ca and Mn in the coatings were higher at longer deposition time. Still, the amount of deposited MnHAp coating was lower than that of HAp coating.

The characteristic fragment ions well representing the HAp moiety were detected in both bioceramic coating layers by TOF SIMS analysis.

The in-vitro degradation rates in Hank's solution were in the sequence: Fe, MnHAp, HAp, from higher to lower. No significant effect of ceramic coating presence on the degradation behavior of iron material was observed, however, the significant increase in biocompatibility is supposed. This will be the scope of further investigation.

ACKNOWLEDGEMENTS
The authors wish to acknowledge financial support from the Projects APVV-0677-11 and APVV-0280-11 of the Slovak Research and Development Agency and Project VEGA 1/0211/12 of the Slovak Scientific Grant Agency.

References

1. B. Ghiban, G. Jicmon and G. Cosmeleata, *Rom. Journ. Phys.* 51 (2006) 187
2. S.M.F. Gad El-Rab, S.A. Fadl-Allah and A.A. Montser, *Appl. Surf. Sci.* 261 (2012) 1
3. S.C. Rizzi, D.J. Heath, A.G.A. Coombes, N. Bock, M. Textor and S. Downes, *J. Biomed. Mater. Res.* 55 (2001) 475
4. M. Schinhammer, I. Gerber, A.C. Hänzi and P.J. Uggowitzer, *Mater. Sci. Eng. C* 33 (2013) 782
5. A.E. Özçam, K.E. Roskov, J. Genzer and R.J. Spontak, *Appl. Mater. Interfaces* 4 (2012) 59
6. B.S. Lee, J.K. Lee, W.J. Kim, Y.H. Jung, S.J. Sim, J. Lee and I.S. Choi, *Biomacromolecules* 8 (2007) 744
7. A. Purnama, H. Hermawan, J. Couet and D. Mantovani, *Acta Biomater.* 6 (2010) 1800
8. A. Oriňák, R. Oriňáková, Z. Orságová Králová, A. Morovská Turoňová, M. Kupková, M. Hrubovčáková, J. Radoňák and R. Džunda, *J. Porous Mater.* 21 (2014) 131
9. M. Peuster, P. Wohlsein, M. Bru¨gmann, M. Ehlerding, K. Seidler, C. Fink, H. Brauer, A. Fischer and G. Hausdorf, *Heart* 86 (2001) 563
10. J. Farack, C. Wolf-Brandstetter, S. Glorius, B. Nies, G. Standke, P. Quadbeck, H. Worch and D. Scharnweber, *Mater. Sci. Eng. B* 176 (2011) 1767
11. B. Liu, Y.F. Zheng and Liquan Ruan, *Mater. Lett.* 65 (2011) 540
12. H. Hermawan, H. Alamdari, D. Mantovani and D. Dube, *Powder Metall.* 51 (2008) 38
13. M.E. Iskandar, A. Aslani and H. Liu, J. *Biomed. Mater. Res.* 101A (2013) 2340
14. A. Yanovska, V. Kuznetsov, A. Stanislavov, S. Danilchenko and L. Sukhodub, *Appl. Surf. Sci.* 258 (2012) 8577
15. J.H. Shepherd, D.V. Shepherd and S.M. Best, *J. Mater. Sci. Mater. Med.* 23 (2012) 2335
16. A. Costan, N. Forna, A. Dima, M. Andronache, C. Roman, V. Manole, L. Stratulat and M. Agop, *J. Optoelectron. Adv. Mater.* 13 (2011) 1338
17. M.F. Ulum, A. Arafat, D. Noviana, A.H. Yusop, A.K. Nasution, M.R. Abdul Kadir and H. Hermawan, *Mater. Sci. Eng. C* 36 (2014) 336
18. N. Eliaz and M. Eliyahu, J. Biomedi. Mater. Res. 80A (2007) 621
19. N. Norziehana Che Isa, Y. Mohd and N. Yury: Electrodeposition of Hydroxyapatite (HAp) Coatings on Etched Titanium Mesh Substrate, 2012 IEEE Colloquium on Humanities, Science & Engineering Research (CHUSER 2012), December 3-4, 2012, Kota Kinabalu, Sabah, Malaysia, p.771 - 775
20. K.Y. Renkema, R.T. Alexander, R.J. Bindels and J.G. Hoenderop, *Ann. Med.* 40 (2008) 82
21. I. Mayer, F.J.G. Cuisinier, S. Gdalya and I. Popov, *J. Inorg. Biochem.* 102 (2008) 311
22. Y. Huang, Q. Ding, S. Han, Y. Yan and X. Pang, *J. Mater. Sci. Mater. Med.* 24 (2013) 1853
23. A. Bigi, B. Bracci, F. Cuisinier, R. Elkaim, M. Fini, I. Mayer, I.N. Mihailescu, G. Socol, L. Sturba and P. Torricelli, *Biomaterials* 26 (2005) 2381
24. E. Gyorgy, P. Toricelli, G. Socol, M. Iliescu, I. Mayer, I.N. Mihailescu, A. Bigi and J. Werckman, J. Biomed. Mater. Res. 71A (2004) 353
25. I. Sopyan, S. Ramesh, N.A. Nawawi, A. Tampieri and S. Sprio, *Ceram. Int.* 27 (2011) 3703
26. B. Bracci, P. Torricelli, S. Panzavolta, E. Boanini, R. Giardino and A. Bigi, *J. Inorg. Biochem.* 103 (2009) 1666
27. Y. Li, J. Widodo, S. Lim and C.P. Ooi, *J. Mater. Sci.* 47 (2012) 754
28. R. Oriňáková, A. Oriňák, L. Markušová Bučková, M. Giretová, Ľ. Medvecký, E. Labbanczová, M. Kupková, M. Hrubovčáková and K. Kovaľ, *Int. J. Electrochem. Sci.* 8 (2013) 12451

29. I. Škugor Rončević, Z. Grubač and M. Metikoš-Huković, *Int. J. Electrochem. Sci.* 9 (2014) 5907
30. Y. Song, S. Zhang, J. Li, C. Zhao and X. Zhang, *Acta Biomater.*, 6 (2010) 1736
31. A. Henss, M. Rohnke, S. Knaack, M. Kleine-Boymann, T. Leichtweiss, P. Schmitz, T. El Khassawna, M. Gelinsky, Christian Heiss and J. Janek, *Biointerphases* 8 (2013) 31
32. N.L. Morozowich, J.O. Lerach, T. Modzelewski, L. Jackson, N. Winograd and H.R. Allcock, *RSC Adv.* 4 (2014) 19680
33. A. Cuneyt Tas F. Korkusuz, M. Timucin and N. Akkas, *J. Mater. Sci. Mater. Med.* 8 (1997) 91
34. R. França, T. Djavanbakht Samani, G. Bayade, L'Hocine Yahia and E. Sachera, *J. Colloid Interface Sci.* 420 (2014) 182